JOURNAL OF Materials CHEMISTRY

Bithiophene–bithiazole copolymers and their metal complexes

Brian J. MacLean and Peter G. Pickup*

Department of Chemistry, Memorial University of Newfoundland, St. John's, Newfoundland, Canada A1B 3X7

Received 29th November 2000, Accepted 18th February 2001
First published as an Advance Article on the web 16th March 2001

This paper describes the synthesis, electrochemistry, and electronic properties of 5,5′-di(2-thienyl)-2,2′-bithiazole, 5,5′-di(2-thienyl)-4,4′-dimethyl-2,2′-bithiazole, and 5,5′-bis(3-methoxy-2-thienyl)-4,4′-dimethyl-2,2′-bithiazole, their complexes with $Ru(bpy)_2^{2+}$ and $Os(bpy)_2^{2+}$, and electrochemically prepared polymer films of these free and complexed ligands. The uncomplexed ligands and their polymers have electrochemical and electronic properties that are similar to the corresponding thiophene homo-oligomers and polymers, with the substituents exhibiting predictable effects. The metal complexes exhibit reversible M(III/II) electrochemistry and ligand based reductions, and can be electrochemically polymerized under suitably anhydrous conditions. BF_3–Et_2O was found to facilitate polymerization, either as the electrochemical solvent or when added to a CH_3CN based solution. The resulting metallopolymers exhibit reversible M(III/II) electrochemistry with no indication of electronic coupling between metal sites. Oxidation of the polymer backbone results in a rapid loss of conjugation, but does not significantly affect the metal and bipyridine based electrochemistry, nor the reductive electrochemistry of the backbone. It is concluded that polymer oxidation is localized on the bithiophene linkages, while its reduction is localized on the bithiazole segments. The evident localization of the backbone π-orbitals is presumed to be responsible for the lack of significant electronic coupling of metal centres through the polymer backbone.

Introduction

The extensive body of research conducted on organic polymers possessing high degrees of π-conjugation has led to the development of new classes of material that are of widespread interdisciplinary interest.[1,2] Interest in these materials lies not only in their processability, but in their exceptional electronic, magnetic and optical properties. Consequently, the scope of applications conceived for these materials is formidable.

Polymers derived from electron-deficient aromatic systems such as pyridine have been developed and have been found to be susceptible to *n*-doping.[3–12] Such materials are anticipated to be useful in the evolution of microelectronics. These polymers are also intriguing in that they can coordinate transition metal ions.[13–19]

2,2′-Bithiazole containing polymers are an interesting example of this class of polymer because of the similarity of the structure of thiazole to thiophene, which is the most commonly used building block for conducting polymers. In fact, a theoretical study[20] has shown that polythiazoles should be good conductors, although experimental studies have failed to confirm this,[21–23] except for bithiophene–bithiazole copolymers.[14,24]

Although polymers incorporating thiazole have been well studied,[7–9,14,20–28] there are few reports of thiazole-based metallopolymers. Wolf and Wrighton have complexed $Re(CO)_3(CH_3CN)^+$ with poly[5,5′-di(2-thienyl)-2,2′-bithiazole-diyl] (poly-**1a**) and demonstrated through changes in the carbonyl stretching frequency that oxidation and reduction of the polymer backbone modulated the electron density at the Re centres. We[29] have reported the electrochemical polymerization of $Os(\mathbf{1a})(bpy)_2^{2+}$ (bpy = 2,2′-bipyridine) to produce a similar type of thiazole-based metallopolymer.

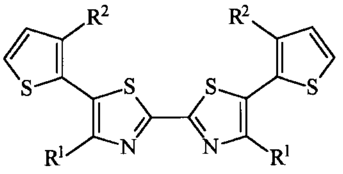

1a $R^1=R^2=H$
1b $R^1=Me, R^2=H$
1c $R^1=Me, R^2=OMe$

Compared with 2,2′-bipyridine based metallopolymers, 2,2′-bithiazole based materials have the potential advantage that they are more easily *p*-doped, and therefore should exhibit stronger d–π electronic interactions with complexed metal ions. This would be expected to lead to more facile electron transport between metal centers with positive formal potentials (such as Ru and Os with polypyridine ligands), and possibly enhanced electrocatalytic activities.

The purpose of this paper is to describe further studies on the synthesis, electrochemistry, and electronic properties of polymers of 5,5′-di(2-thienyl)-2,2′-bithiazole (**1a**), 5,5′-di(2-thienyl)-4,4′-dimethyl-2,2′-bithiazole (**1b**), 5,5′-bis(3-methoxy-2-thienyl)-4,4′-dimethyl-2,2′-bithiazole (**1c**), and to report on the synthesis and electrochemistry of Ru and Os complexes of these ligands and their polymers. The 2,2′-bithiazole moiety present in **1a**, **1b**, and **1c** allows ligation of metal ions directly to the conducting backbone, rather than *via* a tether-type linkage,[30,31] and so should provide more direct interaction between the polymer and the incorporated metal complex. The thiophene end groups of **1a**, **1b** and **1c** are to facilitate anodic polymerization, which is assumed to occur at the thiophene

DOI: 10.1039/b009568k

α-positions,[14,24] and to raise the energy of the valence band (HOMO) to facilitate electron transport between metal (Ru or Os) centres. The methyl substituents on **1b** and **1c**, and the methoxy substitutents on **1c** should raise the valence band still further and a comparison of the strength of the metal–metal interactions in metal complexes of the three polymers (future work) should provide a clear indication of the role of the polymer backbone.

Experimental

Reagents

CH_3CN (spectroscopic grade) was distilled over CaH_2 under Ar before use. Et_4NClO_4 (prepared from Et_4NBr and $HClO_4$) was recrystallized thrice from water and dried under vacuum at 110 °C for 12 h. Bu_4NPF_6 (electrochemical grade, Fluka), CH_2Cl_2 (spectroscopic grade), and all other chemicals were used as received.

Instrumentation

A GE-300NB 300 MHz NMR spectrometer, Hewlett Packard Series 1100 Mass Spectrometer, Cary 5E UV-vis-NIR spectrometer, and Pine Instruments RDE4 potentiostat were used. Atmospheric pressure ionization electrospray (API-ES) mass spectra were recorded for complexes in methanol at a fragmentation voltage of 100 V.

Synthesis

Since Wolf and Wrighton's[14] original synthesis of **1a** based on the Stille coupling of 5,5′-bis(trimethylstannyl)-2,2′-bithiazole with 2-bromothiophene gives poor yields (our best yield was similar to the 9% from bithiazole reported in ref. 14), we investigated two other approaches. The Negishi-type coupling of 5,5′-dibromo-2,2′-bithiazole with 2-thienylzinc chloride, as used in the preparation of **1b** and **1c**,[24] produced insignificant yields, while the Suzuki coupling of 5,5′-dibromo-2,2′-bithiazole and 2-thienylboronic acid (described below) proved to be the best method, producing yields as high as 38% from bithiazole. **1b** and **1c** were prepared by the aforementioned Negishi-type coupling as previously described.[24]

5,5′-Dibromo-2,2′-bithiazole. Br_2 (1.2 cm^3) in $CHCl_3$ (10 cm^3) was slowly added to a stirred solution of 2,2′-bithiazole[32] (1.68 g, 10 mmol) in $CHCl_3$ (200 cm^3). The mixture was heated at reflux under N_2 overnight, followed by washing with dilute $NaHSO_3$ and then water. The organic layer was then dried with $MgSO_4$ and a pale yellow solid was obtained following removal of the solvent. Recrystallization from heavy petroleum ether yielded the product as cream-colored needles (1.47 g, 45%). ^1H NMR (300 MHz, $CDCl_3$, δ (ppm)) 7.75 (s).

5,5′-Di(2-thienyl)-2,2′-bithiazole (1a). 2-Thienylboronic acid[33] (1.56 g, 10 mmol), dissolved in a minimal amount of ethanol, and then 10 cm^3 of a 2 mol dm^{-3} Na_2CO_3 (aq.) were added to a stirred mixture of 5,5′-dibromo-2,2′-bithiazole (1.08 g, 3.3 mmol) and $Pd(PPh_3)_4$ (296 mg) in 1,2-dimethoxyethane (30 cm^3) under N_2. The mixture was then heated at reflux for 18 h, cooled, and filtered. Concentration and purification of the filtrate on a silica–CH_2Cl_2 column, yielded a yellow product (0.93 g, 85%) with a ^1H NMR spectrum in agreement with that reported by Wolf and Wrighton.[14]

Tris(2,2′-bithiazole)ruthenium hexafluorophosphate. [32] A procedure for the synthesis of tris(2,2′-bipyridine)ruthenium chloride was followed.[34] $RuCl_3 \cdot H_2O$ was dried for 3 hours at 130 °C, ground in a mortar, and then dried again for 1 hour. 2,2′-bithiazole (1.00 g, 6 mmol) and $RuCl_3$ (0.45 g, 2 mmol) were then heated to reflux in H_2O, and a solution of phosphinic acid (31%, 2 cm^3) in NaOH (aq.) was added. This mixture was boiled for 2.5 hours, producing a gradual color change from green to brown to reddish brown. The solution was then filtered and a dilute NH_4PF_6 solution was added to the filtrate. The dark red precipitate was collected by filtration and washed well with H_2O (1.64 g, 91%). ^1H NMR (300 MHz, CD_3OD): δ 8.20 (d, $J = 3.0$ Hz, 1H), 7.38 (d, $J = 3.1$ Hz, 1H).

Metal complexes of 1a, 1b, and 1c. Bis(2,2′-bipyridine)ruthenium(II) and bis(2,2′-bipyridine)osmium(II) complexes of **1a**, **1b**, and **1c** were prepared by heating $Ru(bpy)_2Cl_2$[35] or $Os(bpy)_2Cl_2$[35] at reflux with a suspension of the 4-ring ligand in 70% aqueous ethanol (glycerol for Os(**1b**)$(bpy)_2^{2+}$). The progress of the reaction was followed by gel permeation chromatography (Sephadex LH-20–MeOH). When complete, the resulting solution was filtered and $NaClO_4$ (aq.) (or NH_4PF_6 (aq.)) was added to precipitate the metal perchlorate (or hexafluorophosphate) complex. Purification on a Sephadex LH-20–MeOH column afforded products as follows:

*Ru(**1a**)(bpy)₂(ClO₄)₂*. 59% yield; ^1H NMR (300 MHz, CD_3OD): δ 8.68 (d, $J = 8.2$ Hz, 2H), 8.14 (m, 2H), 7.99 (d, $J = 5.7$ Hz, 1H), 7.83 (d, $J = 5.7$ Hz, 1H), 7.64–7.46 (m, 4H), 7.47 (s, 1H), 7.14 (dd, $J = 5.2$, 1.4 Hz, 1H). Electrospray MS (Ru(**1a**)$(bpy)_2(PF_6)_2$): *m/z* 891 (37%, M − PF_6^-), 373 (100%, M − $2PF_6^-$, $z = 2+$).

*Os(**1a**)(bpy)₂(ClO₄)₂*. 67% yield; ^1H NMR (300 MHz, CD_3OD): δ 8.71 (d, $J = 8.1$ Hz, 1H), 8.70 (d, $J = 8.1$ Hz, 1H), 8.03–7.91 (m, 2H), 7.84 (d, $J = 5.7$ Hz, 1H), 7.74 (d, $J = 5.8$ Hz, 1H), 7.62 (d, $J = 5.1$ Hz, 1H), 7.55–7.40 (m, 3H), 7.44 (s, 1H), 7.14 (dd, $J = 5.1$, 1.3 Hz, 1H). Electrospray MS: *m/z* 935 (23%, M − ClO_4^-), 418 (100%, M − $2ClO_4^-$, $z = 2+$).

*Ru(**1b**)(bpy)₂(ClO₄)₂*. 83% yield; ^1H NMR (300 MHz, CD_3OD): δ 8.74 (d, $J = 8.1$ Hz, 1H), 8.67 (d, $J = 8.2$ Hz, 1H), 8.22 (t, $J = 7.9$, 1H), 8.14 (d, $J = 5.5$ Hz, 1H), 8.07 (t, $J = 7.9$ Hz, 1H), 7.78 (d, $J = 5.5$ Hz, 1H), 7.71–7.63 (m, 2H), 7.44–7.36 (m, 2H), 7.19 (dd, $J = 5.2$, 1.5 Hz, 1H), 1.73 (s, 3H). Electrospray MS (Ru(**1b**)$(bpy)_2(PF_6)_2$): *m/z* 387 (100%, M − $2PF_6^-$, $z = 2+$), 360 (**1b**).

The structure of this complex was confirmed by X-ray crystallography. CCDC 157031. See http://www.rsc.org/suppdata/jm/b0/b009568k/ for crystallographic files in .cif format.

*Os(**1b**)(bpy)₂(ClO₄)₂*. 71% yield; ^1H NMR (300 MHz, CD_3OD): δ 8.69 (d, $J = 8.0$ Hz, 1H), 8.66 (d, $J = 8.3$ Hz, 1H), 7.99 (t, $J = 8.0$ Hz, 1H), 7.93 (d, $J = 5.7$ Hz, 1H), 7.86 (t, $J = 7.8$ Hz, 1H), 7.68 (d, $J = 5.2$ Hz, 1H), 7.63 (d, $J = 5.6$ Hz, 1H), 7.56 (t, $J = 6.7$ Hz, 1H), 7.39–7.33 (m, 2H), 7.18 (dd, $J = 5.2$, 1.4 Hz, 1H), 1.74 (s, 3H). Electrospray MS (at 150 V): *m/z* 963 (13%, M − ClO_4^-), 951 (70%), 864 (6%, M − $2ClO_4^-$, $z = 1+$), 432 (70%, M − $2ClO_4^-$, $z = 2+$), 360 (100%, **1b**).

*Ru(**1c**)(bpy)₂(ClO₄)₂*. 39% yield; ^1H NMR (300 MHz, CD_3OD): δ 8.73 (d, $J = 8.2$ Hz, 1H), 8.67 (d, $J = 8.0$ Hz, 1H), 8.18 (t, $J = 7.6$ Hz, 1H), 8.07 (m, 2H), 7.80 (d, $J = 5.9$ Hz, 1H), 7.67–7.59 (m, 2H), 7.41 (t, $J = 6.6$ Hz, 1H), 7.15 (d, $J = 5.4$ Hz, 1H), 4.03 (s, 3H), 1.75 (s, 3H). Electrospray MS (Ru(**1c**)$(bpy)_2Cl_2$ prepared by ion-exchange): *m/z* 477 (100%), 441 (45%), 414 (24%, $Ru(bpy)_2^+$). Electrospray MS of the perchlorate salt of this complex also failed to yield ions that could be identified as containing intact **1c**. Prominent peaks at $m/z = 441$ and 477 were also observed for Ru(4,4′-dimethyl-2,2′-bithiazole)$(bpy)_2(ClO_4)_2$.

A small quantity of Os(**1c**)$(bpy)_2(ClO_4)_2$ was also prepared (19% yield), but was not satisfactorily characterized. Cyclic voltammetry (Table 1) was consistent with the proposed formula, although no ligand oxidation wave was observed.

Table 1 Formal potentials (V *vs.* SSCE) from cyclic voltammograms of the monomers (in CH_2Cl_2) and their complexes (in CH_3CN)

Compound	Oxidation of **1**[a]	M(III/II)	Reduction of **1**	Other ligand based reductions		
1a	1.36		−1.65			
1b	1.30		−1.65			
1c	0.94		−1.63			
Ru(**1a**)$(bpy)_2(ClO_4)_2$	1.58	1.24	−0.88		−1.64	−1.85
Ru(**1b**)$(bpy)_2(ClO_4)_2$	1.60	1.29	−0.97		−1.47	−1.64
Ru(**1c**)$(bpy)_2(ClO_4)_2$	1.64	1.17	−1.05		−1.47	−1.71
$Ru(bpy)_3(ClO_4)_2$		1.27		−1.31	−1.51	−1.73
$Ru(btz)_3(PF_6)_2$		1.33		−1.04	−1.23	−1.44
Os(**1a**)$(bpy)_2(ClO_4)_2$	1.65	0.84	−0.89		−1.31	−1.63
Os(**1b**)$(bpy)_2(ClO_4)_2$	1.69	0.86	−0.92		−1.35	−1.60
Os(**1c**)$(bpy)_2(ClO_4)_2$[b]	>2V	0.85	−1.04		−1.42	−1.70
$Os(bpy)_3^{2+}$ (ref. 46)		0.82		−1.26	−1.45	−1.76

[a]Anodic peak potential. [b]Sample not characterized; no ligand oxidation wave observed. btz = 2,2′-bithiazole.

Electrochemistry

Electrochemical experiments were conducted in conventional cells under an argon atmosphere, with Pt disc working electrodes (5×10^{-3} cm^2) and an SSCE reference electrode. All potentials are quoted with respect to the SSCE.

Electrochemical polymerization of 1a, 1b, and 1c. The electrochemical formation of films of poly-**1a**,[14] poly-**1b**,[24] and poly-**1c**[24] on electrodes has previously been reported. In this work, films were formed from a solution of the monomer in $CHCl_3$ (or CH_2Cl_2)–Bu_4NPF_6 by repetitive scanning of the potential (at 100 mV s^{-1}) between 0 and +1.4 V for **1a** (in CH_2Cl_2–Bu_4NPF_6), 0 and +1.3 V for **1b**, and 0 and +1.0 V for **1c**.

Results and discussion

Monomer properties

Tables 1 and 2 summarize voltammetric and UV-visible spectroscopic data for the three monomers and their $Ru(bpy)_2^{2+}$ and $Os(bpy)_2^{2+}$ complexes.

Comparing the anodic peak potentials for oxidation of **1a**, **1b** and **1c** it can be seen that the methyl substituents make the molecule slightly easier to oxidize while the methoxy substituents have a much larger stabilizing effect on the oxidized form. Formal potentials for reductions are virtually unchanged by substitution. The oxidation of **1c** at 0.94 V was preceded by a small prepeak at 0.73 V, as previously observed.[24] Cycling through this peak led to polymer formation, and so we speculate that it is due to adsorbed **1c**.

λ_{max} values from UV-visible spectroscopy (Table 2) are only slightly affected by substitution. They are all slightly higher than that of quaterthiophene (390 nm[36]).

Dissolution of **1a**, **1b**, or **1c** in acid brings about a large red-shift in their UV-visible spectrum, as illustrated in Fig. 1 for **1a**. This dramatic (*ca.* 0.3 eV) decrease in the HOMO–LUMO gap upon protonation can be qualitatively modeled by semiempirical calculations at the AM1 level (the calculations were performed using SPARTAN from Wavefunction, Inc.). Diprotonation of **1a**, for example, causes the calculated HOMO and LUMO energies to decrease by ~5.6 and ~7.2 eV, respectively, corresponding to a *ca.* 1.6 eV reduction in the HOMO–LUMO gap. The differences in experimental values would be expected to be smaller than this because of solvation of the protonated form and the presence of counter ions.

Complexation of a $M(bpy)_2$ moiety to any of the monomers produces voltammograms (*e.g.* Fig. 2) dominated by the electrochemistry of the metal complex. The M(III/II) wave occurs at a formal potential close to that of the corresponding $M(bpy)_3^{2+}$ complex (Table 1), while the first ligand reduction wave is shifted significantly positive relative to that of the corresponding $M(bpy)_3^{2+}$ complex, and appears close to or more positive than the first ligand reduction wave for

Table 2 UV-visible spectroscopic data for the monomers (π→π* transition in CH_2Cl_2) and their complexes (MLCT in CH_3CN)

	λ_{max}/nm	
Compound	Ligand	MLCT
1a	404	—
1b	398	—
1c	418	—
Ru(**1a**)$(bpy)_2(ClO_4)_2$	429	492
Ru(**1b**)$(bpy)_2(ClO_4)_2$	423	480
Os(**1a**)$(bpy)_2(ClO_4)_2$	422	519
Os(**1b**)$(bpy)_2(ClO_4)_2$	430	510

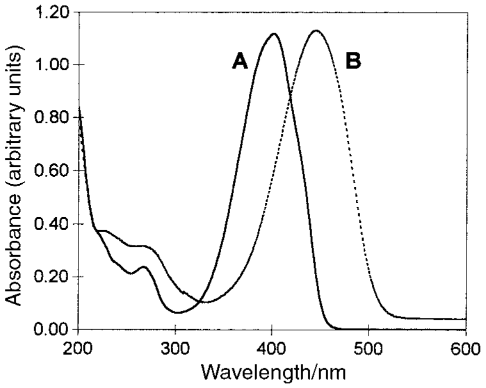

Fig. 1 UV-vis spectra of **1a** in CH_3CN (A) and CH_3CN containing $HClO_4$ (B).

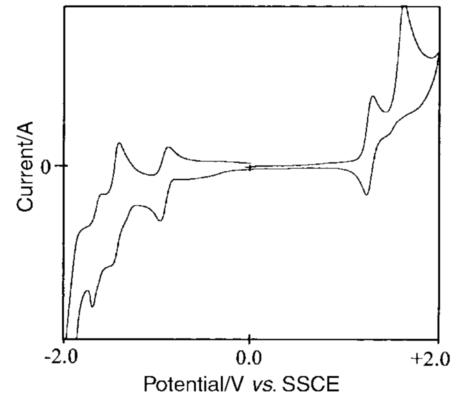

Fig. 2 Cyclic voltammogram (100 mV s^{-1}) of Ru(**1a**)$(bpy)_2(ClO_4)_2$ (*ca.* 9 mM) in CH_3CN containing 0.1 mol dm^{-3} Et_4NClO_4.

$Ru(btz)_3^{2+}$. This reduction can therefore be assigned to the di(thienyl)bithiazole ligand. The other two reduction waves occur at formal potentials close to those of the corresponding $M(bpy)_3^{2+}$ complex, and so can be assigned to reductions based on the two bipyridine ligands.

In the UV-vis spectra (Table 2), the di(thienyl)bithiazole ligand absorption is shifted significantly to higher wavelength, consistent with the electron withdrawing effect of the metal which will affect the LUMO more than the HOMO, as demonstrated above for protonation. The metal to ligand charge transfer bands appear at significantly higher wavelengths relative to the $M(bpy)_3^{2+}$ complexes. Since the metal (III/II) potentials are not greatly different, this indicates that the di(thienyl)bithiazole ligands have relatively low lying LUMOs, and is consistent with their relative ease of reduction (Table 1).

Doping potentials and band gaps of poly-1a, poly-1b, and poly-1c

Fig. 3 shows two examples of cyclic voltammograms of poly-**1a** films. For the solid curve, the potential was initially scanned in the positive (anodic) direction. An anodic current attributable to *p*-doping of the polymer commences at *ca.* +0.7 V and continues to rise to the chosen anodic potential limit of +1.6 V (this limit is sufficient to cause complete degradation of the polymer within a few cycles). Two un-doping peaks are seen at +1.28 and +0.84 V on the reverse scan, and then *n*-doping commences at *ca.* −1.2 V. The *n*-doping/un-doping waves consist of a prepeak at −1.44 V and cathodic and anodic peaks at a formal potential of −1.57 V. When the potential is initially scanned negatively (Fig. 3, dashed curve), *n*-doping begins somewhat later but the un-doping peak is not shifted significantly. On the anodic scan, *p*-doping commences earlier (*ca.* +0.45 V), with a prepeak at +0.66 V, and a reversible *p*-doping wave is seen at a formal potential of +1.23 V. The differences between the two curves in Fig. 3 can be attributed primarily to ion transport effects, whereby the electrochemistry of the film becomes more facile after ions and solvent have been brought into the film by the first oxidation or reduction.

Both voltammograms in Fig. 3 have small anodic and cathodic waves at $E^{o'} \sim -0.27$ V, that are incompatible with the expected structure of the polymer (α–α linkage of the terminal thiophene units). However, this feature can probably be assigned to *n*-doping/un-doping of protonated segments of the polymer.[37]

Cyclic voltammograms of poly-**1b** and poly-**1c** are similar to those of poly-**1a**, and pertinent data are presented in Table 3. Both the methyl and methoxy substituents significantly decrease the formal potential for oxidation, consistent with their electron donating effects. The formal potentials for reduction are less affected, with the methyl groups in **1b** causing an insignificant positive shift, and the methoxy groups in **1c** causing a slight negative shift The consequence of this is that the substituted polymers, particularly poly-**1c**, have significantly lower band gaps than poly-**1a**. However, the complex voltammograms observed (*e.g.* Fig. 3), and uneven baselines in UV-vis spectra of the polymers, have prevented us from accurately determining band gaps.

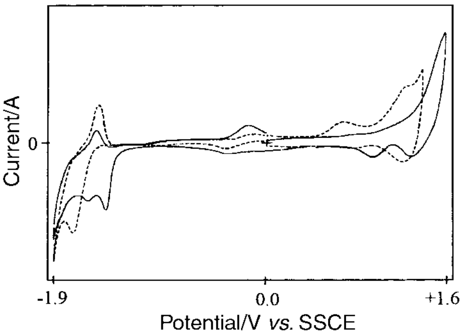

Fig. 3 Cyclic voltammograms (100 mV s^{-1}) of poly-**1a** films in CH_2Cl_2 containing 0.1 mol dm^{-3} Bu_4NPF_6. Solid line: initial scan direction positive; dashed line: initial scan direction negative.

Table 3 Electrochemical (in CH_2Cl_2) data for poly-**1** films

Polymer	$E^{o'}$ (*p*-doping)/V	$E^{o'}$ (*n*-doping)/V
Poly-**1a**	+1.23	−1.57
Poly-**1b**	~+0.9	−1.52
Poly-**1c**	+0.40	−1.71

The electronic structure of the 4 ring system is seen to be markedly affected by polymerization, as corresponding redox potentials for the monomer are significantly more separated (Table 1). The decrease in the gap between oxidation and reduction attests to increased delocalization over a larger π-skeleton in the polymers.

The polymers are not soluble in common organic solvents but dissolve in concentrated acids to give deep blue solutions. UV-visible spectra (*e.g.* Fig. 4) show a large shift of the π–π* peak to higher wavelength (from 404 to 653 nm for poly-**1a**). This dramatic decrease in band gap upon protonation parallels the decrease in the HOMO–LUMO gap observed for the monomer.

Preparation of metallopolymers

Surprisingly, we have found that none of the metal complexes listed in Table 1 give sustained polymer film growth on the electrode when the potential is cycled through the di(thienyl)bithiazole ligand wave in CH_3CN, the most common solvent for electrochemical polymerizations. However, Os(**1a**)$(bpy)_2(ClO_4)_2$ can be polymerized by cycling repeatedly through the ligand oxidation wave at *ca.* +1.65 V in a $CH_3CN + Et_4NClO_4$ solution containing BF_3–Et_2O.[29] It appears that the high potentials required to oxidize the di(thienyl)bithiazole ligand, combined with the limited concentrations (*ca.* 10 mM) of complex that can be used, results in destruction of the growing polymer's conjugated backbone by trace water in the system. Addition of BF_3–Et_2O to sequester water solves this problem for Os(**1a**)$(bpy)_2(ClO_4)_2$, but has not been successful for any of the other complexes listed in Table 1. Ru(**1a**)$(bpy)_2(ClO_4)_2$, Ru(**1b**)$(bpy)_2(ClO_4)_2$ and Os(**1b**)$(bpy)_2(ClO_4)_2$ have however been successfully polymerized in neat BF_3–Et_2O[38] (polymerization of Os(**1a**)$(bpy)_2(ClO_4)_2$ was not attempted under these conditions). The polymerization of Ru(**1a**)$(bpy)_2(ClO_4)_2$ is illustrated in Fig. 5. In these voltammograms, the Ru(III/II) wave of the complex appears at a formal potential of *ca.* +1.0 V while the di(thienyl)bithiazole ligand wave peaks at *ca.* 1.4 V. Repeated cycling through the ligand oxidation wave

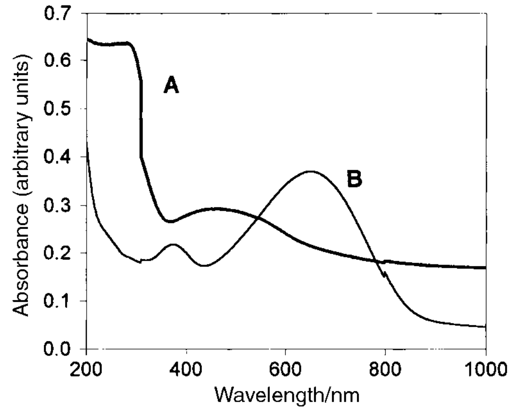

Fig. 4 UV-vis spectra of poly-**1a** on an ITO electrode (A) and dissolved in conc. H_2SO_4 (B).

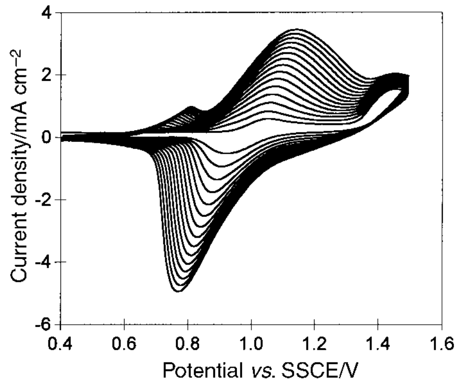

Fig. 5 Cyclic voltammograms (100 mV s^{-1}) of Ru(**1a**)(bpy)$_2$(ClO$_4$)$_2$ (5 mmol dm^{-3}) in BF$_3$–Et$_2$O. All peaks increased with cycling.

produces a rapid increase in the Ru(III/II) waves that is indicative of polymer deposition on the electrode.

Use of BF$_3$–Et$_2$O, either neat or added to more conventional electrolyte solutions, does not allow polymerization of Ru(**1c**)(bpy)$_2$(ClO$_4$)$_2$ because of complexation of BF$_3$ with the methoxy groups of the ligand. However, although homopolymers of Ru(**1c**)(bpy)$_2$(ClO$_4$)$_2$ could not be prepared, copolymers with 2,2′-bithiophene were obtained. Thin poly[Ru(**1c**)(bpy)$_2$(ClO$_4$)$_2$-*co*-(2,2′-bithiophene)] films were prepared by cycling the potential of a Pt electrode between 0.5 and 1.5 or 1.6 V in solutions containing *ca.* 1–5 mM of the metal complex and 0.2–0.6 mM bithiophene.

Metallopolymers

Poly[Ru(1a)(bpy)$_2$(ClO$_4$)$_2$]. Figs. 6 and 7 show cyclic voltammograms of a poly[Ru(**1a**)(bpy)$_2$(ClO$_4$)$_2$] coated Pt electrode in CH$_3$CN containing Bu$_4$NPF$_4$. The anodic electrochemistry of poly[Ru(**1a**)(bpy)$_2$(ClO$_4$)$_2$] (Fig. 6) involves a reversible Ru(III/II) wave at +1.43 V and an irreversible oxidation wave at +1.75 V, that appears only on the first scan. The latter can be attributed to overoxidation[39] of the polymer backbone. The small wave at *ca.* +0.2 V in Fig. 6, which appears only at the end of the first scan is presumably due to H$^+$ produced in the overoxidation process.

There are several surprising features of this anodic electrochemistry. Firstly, the wave that we have attributed to the backbone occurs at a higher potential than the Ru(III/II) wave, while for an analogous polymer based on di(dithienyl)bipyridine[40] it occurs below the Ru(III/II) wave. The fewer thiophene units in the linkage in poly[Ru(**1a**)(bpy)$_2$(ClO$_4$)$_2$] (2 *vs.* 4 in poly(Ru{5,5′-di[5-(2,2′-bithienyl)-2,2′-bipyridine](bpy)$_2$-(ClO$_4$)$_2$})) clearly produce a less electron rich backbone. It is also surprising that the Ru(III/II) wave is not split or broadened by electronic coupling between adjacent Ru sites through the polymer backbone. Strong coupling through a hole superexchange mechanism might be expected in light of the proximity of the metal and ligand waves. However, it would appear that the polymer HOMO is too localized on the bithienyl segments of the backbone to facilitate strong coupling. The lack of significant intermetal coupling in poly[Ru(**1a**)(bpy)$_2$$^{2+}$] is consistent with a similar lack of coupling recently reported for a thiophene-2,5-diyl bridged binuclear Ru(terpy)$_2$$^{2+}$-based complex.[41] Steric factors may also play a role in localizing the HOMO in the polymers studied here.

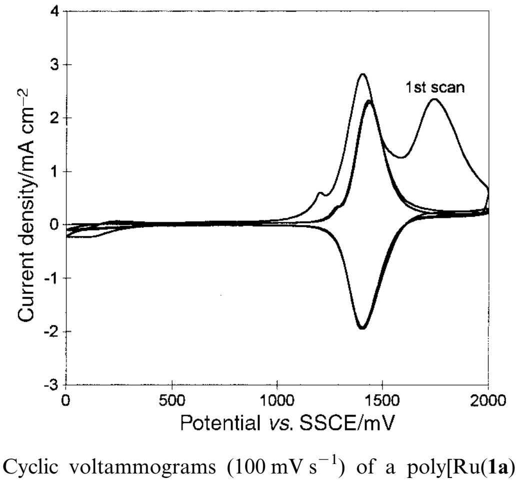

Fig. 6 Cyclic voltammograms (100 mV s^{-1}) of a poly[Ru(**1a**)(bpy)$_2$-(ClO$_4$)$_2$] coated Pt electrode in CH$_3$CN containing 0.1 mol dm^{-3} Bu$_4$NPF$_6$.

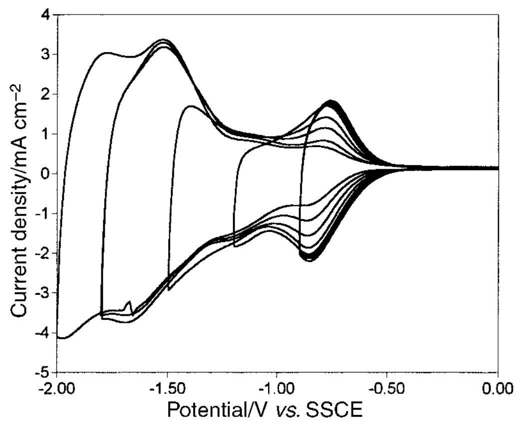

Fig. 7 Cyclic voltammograms (100 mV s^{-1}) of a poly[Ru(**1a**)(bpy)$_2$-(ClO$_4$)$_2$] coated Pt electrode in CH$_3$CN containing 0.1 mol dm^{-3} Bu$_4$NPF$_6$. The first 6 scans were to −0.9 V, and then the lower potential limit was decreased successively to −2.0 V.

Reduction of poly[Ru(**1a**)(bpy)$_2$(ClO$_4$)$_2$] occurs in four reversible steps (Fig. 7). Based on the assignments made for the monomer complexes, the larger waves at formal potentials of −1.60 and −1.87 V are due to the two bipyridine ligands. The smaller, most positive wave at $E^{o'} = -0.80$ V must be due to *n*-doping (reduction) of the polymer backbone. The yet smaller (or broader) wave at $E^{o'} = -1.16$ V may also be a backbone reduction. The polymer wave at −0.8 V is reasonably stable to potential cycling as long as the potential is kept above −1 V, however, cycling to lower potentials causes it to decay, indicating that the conjugated backbone of the polymer is being degraded. The bipyridine waves are unaffected by this, and so the polymer film must remain intact on the electrode.

The electrochemistry of poly[Ru(**1b**)(bpy)$_2$(ClO$_4$)$_2$] is very similar to that described above for poly[Ru(**1a**)(bpy)$_2$(ClO$_4$)$_2$].

Poly[Os(1a)(bpy)$_2$(ClO$_4$)$_2$]. Fig. 8 shows cyclic voltammograms of a poly[Os(**1a**)(bpy)$_2$(ClO$_4$)$_2$] coated Pt electrode. The anodic electrochemistry shows only a single reversible Os(III/II) wave at $E^{o'} = +0.87$ V, with no polymer wave at higher potentials. Presumably, the conjugation in the backbone was destroyed during the polymerization. It is likely that a poly[Os(**1a**)(bpy)$_2$(ClO$_4$)$_2$] (or poly[Os(**1b**)(bpy)$_2$(ClO$_4$)$_2$]) film prepared from neat BF$_3$–Et$_2$O would exhibit a transient polymer oxidation wave, as described above for poly[Ru(**1a**)-(bpy)$_2$(ClO$_4$)$_2$], but this was not investigated because of the limited quantities of the Os complexes that were available.

The cathodic electrochemistry of poly[Os(**1a**)(bpy)$_2$-(ClO$_4$)$_2$][29] is very similar to that of poly[Ru(**1a**)(bpy)$_2$(ClO$_4$)$_2$] shown in Fig. 7. A polymer reduction wave appears at $E^{o'} = -0.79$ V, and there are bipyridine reductions at $E^{o'} = -1.62$ and −1.85 V. The appearance of a polymer reduction wave when no polymer oxidation is observed might appear to be contradictory. However, the polymer reduction would be expected to be localized on the bithiazole

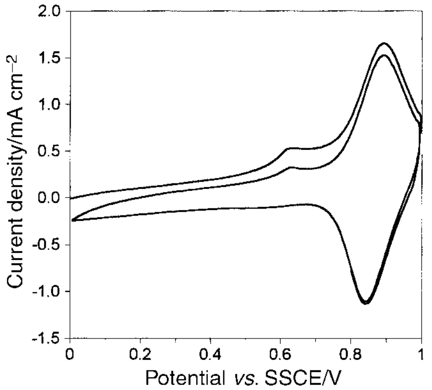

Fig. 8 Cyclic voltammograms (100 mV s^{-1}) of a poly[Os(**1a**)(bpy)$_2$(ClO$_4$)$_2$] coated Pt electrode in CH$_3$CN containing 0.1 mol dm^{-3} Et$_4$NClO$_4$.

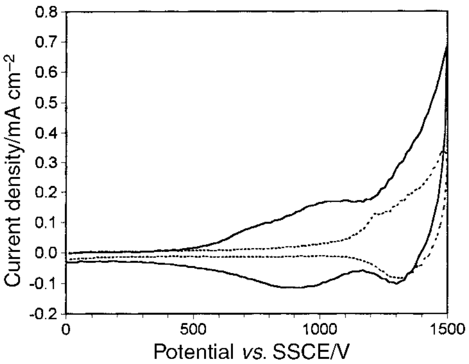

Fig. 9 Cyclic voltammograms (100 mV s^{-1}) of a poly[Ru(**1c**)(bpy)$_2$(ClO$_4$)$_2$-*co*-(2,2′-bithiophene)] coated electrode in CH$_3$CN containing 0.1 mol dm^{-3} Bu$_4$NPF$_6$, before (solid) and after (dashed) impedance experiments.

segments, while the oxidation should be localized on the bithiophene linkages.[42] During overoxidation, the backbone would be attacked by trace water at the bithiophene linkages, thereby deactivating its anodic but not cathodic electrochemistry.

Poly[Ru(1c)(bpy)$_2$(ClO$_4$)$_2$-*co*-(2,2′-bithiophene)]. Fig. 9 shows cyclic voltammograms of a poly[Ru(**1c**)(bpy)$_2$(ClO$_4$)$_2$-*co*-(2,2′-bithiophene)] coated electrode. The broad wave at *ca.* 1.0 V indicates that a conjugated backbone has been formed, with the sharper wave at *ca.* 1.3 V indicating that the film contains the intact Ru centre of the original complex. Both waves are reasonably stable to repeated cycling, although the lower potential one does decrease gradually. Holding the potential at +1.3 V for *ca.* 20 min (in impedance experiments) resulted in complete loss of the wave at *ca.* 1.0 V, while the Ru wave remained virtually unchanged. It would thus appear that the conjugated backbone is quite susceptible to attack by trace water. The retention of the Ru wave suggests that the complex is covalently bound into the film, rather than simply trapped by steric restraints. Impedance spectroscopy[43] at the Ru formal potential indicated that electron hopping between Ru sites in the polymer was very slow (the electron diffusion coefficient, D_e, was only *ca.* 10^{-10} cm^2 s^{-1}). The conjugated backbone does not therefore appear to enhance the rate of electron transport between Ru sites over values in non-conjugated polymers.[43]

Conclusions

The main goals of this work were to produce metallopolymers with electronic coupling between metal sites. It is significant therefore that neither poly[Ru(**1a**)(bpy)$_2$(ClO$_4$)$_2$], poly[Os(**1a**)(bpy)$_2$(ClO$_4$)$_2$], nor poly[Ru(**1c**)(bpy)$_2$(ClO$_4$)$_2$-*co*-(2,2′-bithiophene)] show any splitting or broadening of the M(III/II) wave that would be indicative of electronic coupling between metal sites. The properties of the uncomplexed polymers, which are similar to those of polythiophene, would suggest that strong coupling through the polymer HOMO would be possible, and energetically this type of interaction would be expected in the metallopolymers. The lack of significant electronic coupling of metal centres through the polymer backbone can be attributed to localization of the backbone π-orbitals, as indicated by the electrochemical behaviour of the metallopolymers. To achieve electronic interactions between metal centers through a conjugated polymer, it is clearly necessary to match the energy levels of the coordinating and linking segments. This has been done in polybenzimidazole based metallopolymers,[43–45] where the benzimidazole, pyridine, and pyrazine based linkages are more electron deficient than the bithiophenes used here. It would appear that future materials should combine the relatively electron rich bithiazole ligand with linkages that are more electron deficient than bithiophene.

Acknowledgement

This work was supported by the Natural Sciences and Engineering Research Council of Canada and Memorial University. We thank Dr Ieuan Jenkins for preparing **1b** and **1c**. We thank Dr Bob McDonald, University of Alberta, for collecting X-ray data for Ru(**1b**)(bpy)$_2$(ClO$_4$)$_2$ and David O. Miller for solving/refining this data.

References

1 T. A. Skotheim, R. L. Elsenbaumer and J. R. Reynolds, eds., *Handbook of Conducting Polymers*, 2nd edn., Mercal Dekker, New York, 1998.
2 I. B. Bersuker, *Electronic structure and properties of transition metal compounds: introduction to the theory*, Wiley, New York, 1996.
3 T. Yamamoto, T. Ito and K. Sanechika, *Synth. Met.*, 1988, **25**, 103.
4 S. Janietz and B. Schulz, *Eur. Polym. J.*, 1996, **32**, 465.
5 T. Yamamoto, *J. Polym. Sci., Part A, Polym. Chem.*, 1996, **34**, 997.
6 A. K. Agrawal and S. A. Jenekhe, *Chem. Mater.*, 1996, **8**, 579.
7 M. D. Curtis, H. T. Cheng, J. A. Johnson, J. I. Nanos, R. Kasim, R. L. Elsenbaumer, L. G. Ronda and D. C. Martin, *Chem. Mater.*, 1998, **10**, 13.
8 M. D. Curtis, H. T. Cheng, J. I. Nanos and G. A. Nazri, *Macromolecules*, 1998, **31**, 205.
9 J. K. Politis, M. D. Curtis, L. Gonzalez, D. C. Martin, Y. He and J. Kanicki, *Chem. Mater.*, 1998, **10**, 1713.
10 I. H. Jenkins, U. Salzner and P. G. Pickup, *Chem. Mater.*, 1996, **8**, 2444.
11 I. H. Jenkins, N. G. Rees and P. G. Pickup, *Chem. Mater.*, 1997, **9**, 1213.
12 T. Yamamoto, T. Maruyama, Z.-H. Zhou, T. Ito, T. Fukuda, Y. Yoneda, F. Begum, T. Ikeda, S. Sasaki, H. Takezoe, A. Fukuda and K. Kubota, *J. Am. Chem. Soc.*, 1994, **116**, 4832.
13 T. Yamamoto, Y. Yoneda and T. Maruyama, *Chem. Commun.*, 1992, 1652.
14 M. O. Wolf and M. S. Wrighton, *Chem. Mater.*, 1994, **6**, 1526.
15 T. Maruyama and T. Yamamoto, *Inorg. Chim. Acta.*, 1995, **238**, 9.
16 S. C. Rasmussen, D. W. Thompson, V. Singh and J. D. Petersen, *Inorg. Chem.*, 1996, **35**, 3449.
17 S. S. Zhu and T. M. Swager, *Adv. Mater.*, 1996, **8**, 497.
18 S. S. Zhu, P. J. Carroll and T. M. Swager, *J. Am. Chem. Soc.*, 1996, **118**, 8713.
19 S. S. Zhu and T. M. Swager, *J. Am. Chem. Soc.*, 1997, **119**, 12568.
20 M. Catellani, S. Destri, W. Porzio, B. Themans and J. L. Bredas, *Synth. Met.*, 1988, **26**, 259.
21 A. Bolognesi, M. Catellani, S. Destri and W. Porzio, *Syntht. Met.*, 1987, **18**, 129.

22 T. Maruyama, H. Suganuma and T. Yamamoto, *Synth. Met.*, 1995, **74**, 183.

23 T. Yamamoto, H. Suganuma, T. Maruyama and K. Kubota, *Chem. Commun.*, 1995, 1613.

24 I. H. Jenkins and P. G. Pickup, *Macromolecules*, 1993, **26**, 4450.

25 S. Tanaka and K. Kaeriyama, *Makromol. Chem., Rapid Commun.*, 1988, **9**, 743.

26 J. I. Nanos, J. W. Kampf and M. D. Curtis, *Chem. Mater.*, 1995, **7**, 2232.

27 T. Yamamoto, H. Suganuma, T. Maruyama, T. Inoue, Y. Muramatsu, M. Arai, D. Komarudin, N. Ooba, S. Tomaru, S. Sasaki and K. Kubota, *Chem. Mater.*, 1997, **9**, 1217.

28 T. Yamamoto, D. Komarudin, M. Arai, B. L. Lee, H. Suganuma, N. Asakawa, Y. Inoue, K. Kubota, S. Sasaki, T. Fukuda and H. Matsuda, *J. Am. Chem. Soc.*, 1998, **120**, 2047.

29 B. J. MacLean and P. G. Pickup, *Chem. Commun.*, 1999, 2471.

30 S. J. Higgins, *Chem. Soc. Rev.*, 1997, **26**, 247.

31 A. Deronzier and J.-C. Moutet, *Coord. Chem. Rev.*, 1996, **147**, 339.

32 G. Orellana, C. Alvarez-Ibarra and M. L. Quiroga, *Bull. Soc. Chim. Belg.*, 1988, **97**, 731.

33 A.-B. Hornfeldt and S. Gronowitz, *Ark. Kemi.*, 1963, **21**, 239.

34 J. A. Broomhead and C. G. Young, *Inorg. Synth.*, 1982, **21**, 127.

35 P. A. Lay, A. M. Sargeson and H. Taube, *Inorg. Synth.*, 1986, **24**, 291.

36 H. Chosrovian, D. Grebner, S. Rentsch and H. Naarman, *Synth. Met.*, 1992, **52**, 213.

37 G. Zotti, S. Zecchin, G. Schiavon, A. Berlin and M. Penso, *Chem. Mater.*, 1999, **11**, 3342.

38 G. Q. Shi, C. Li and Y. Q. Liang, *Adv. Mater.*, 1999, **11**, 1145.

39 A. A. Pud, *Synth. Met.*, 1994, **66**, 1.

40 S. S. Zhu, R. P. Kingsborough and T. M. Swager, *J. Mater. Chem.*, 1999, **9**, 2123.

41 E. C. Constable, C. E. Housecroft, E. R. Schofield, S. Encinas, N. Armaroli, F. Barigelletti, L. Flamigni, E. Figgemeier and J. G. Vos, *Chem. Commun.*, 1999, 869.

42 P. G. Pickup, *J. Mater. Chem.*, 1999, **8**, 1641.

43 C. G. Cameron and P. G. Pickup, *J. Am. Chem. Soc.*, 1999, **121**, 11773.

44 C. G. Cameron and P. G. Pickup, *Chem. Commun.*, 1997, 303.

45 C. G. Cameron and P. G. Pickup, *J. Am. Chem. Soc.*, 1999, **121**, 7710.

46 H. D. Abruna, *J. Electroanal. Chem.*, 1984, **175**, 321.